JACS
JOURNAL OF THE AMERICAN CHEMICAL SOCIETY
pubs.acs.org/JACS
Article

[8+2] vs [4+2] Cycloadditions of Cyclohexadienamines to Tropone and Heptafulvenes—Mechanisms and Selectivities

Xiangyang Chen,[†] Mathias Kirk Thøgersen,[†] Limin Yang, Rune F. Lauridsen, Xiao-Song Xue, Karl Anker Jørgensen,* and K. N. Houk*

Cite This: *J. Am. Chem. Soc.* 2021, 143, 934−944

ABSTRACT: The cinchona-alkaloid-catalyzed cycloaddition reactions of 2-cyclohexenone with tropone and various heptafulvenes give [8+2] or [4+2] cycloadducts, depending on the substituents present on the heptafulvene. We report the results of new experiments with heptafulvenes, containing diester and barbiturate substituents, which in combination with computational studies were performed to elucidate the factors controlling [8+2] vs [4+2] cycloaddition pathways, including chemo-, regio-, and stereoselectivities of these higher-order cycloadditions. The protonated cinchona alkaloid primary amine catalyst reacts with 2-cyclohexenone to form a linear dienamine intermediate that subsequently undergoes a stepwise [8+2] or [4+2] cycloaddition. Both tropone and the different heptafulvenes initially form [8+2] cycloadducts. The final product is ultimately decided by the reversibility of the [8+2] cycloaddition and the relative thermal stability of the [4+2] products. The stereoisomeric transition states are distinguished by the steric interactions between the protonated catalyst and tropone/heptafulvenes. The [8+2] cycloaddition of barbiturate-heptafulvene afforded products with an unprecedented *trans*-fusion of the five- and six-membered rings, while the [8+2] cycloadducts obtained from cyanoester-heptafulvene and diester-heptafulvene were formed with a *cis*-relationship. The mechanism, thermodynamics, and origins of stereoselectivity were explained through DFT calculations using the ωB97X-D density functional.

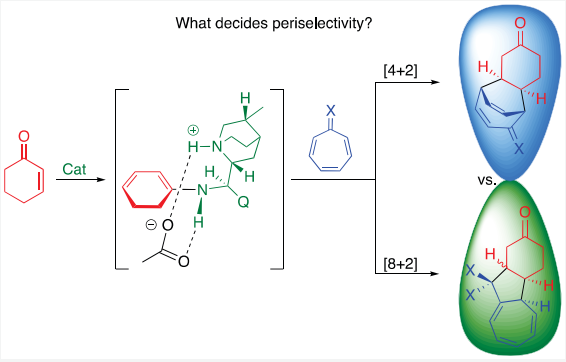

INTRODUCTION

Cycloadditions are among the most useful reactions in organic chemistry. Characterized by high functional group tolerance and excellent stereocontrol, the prototypical Diels−Alder [4+2] cycloaddition has found numerous synthetic applications in the construction of six-membered ring systems.[1] Building upon the theoretical considerations introduced by Woodward and Hoffmann,[2] countless experimental and computational studies have focused on elucidating the mechanisms and selectivities of various [4+2] cycloadditions.[3]

Cycloadditions involving more than six π-electrons are less well-studied and much more challenging to control. Useful applications of such higher-order cycloadditions in natural product syntheses have been hampered by inadequate control of regioselectivity, *endo*/*exo*-diastereoselectivity, and facial stereoselectivity. Periselectivity (or chemoselectivity when the reactions are stepwise) poses an additional challenge, as extended polyene systems—such as tropone—are known to participate in competing cycloadditions involving a varying number of its π-electrons, often leading to complex product mixtures.[4] Previously, metal templates have been utilized to restrict the conformational flexibility of the polyene and suppress undesired reaction paths.[5]

More recently, asymmetric organocatalysis has allowed for the development of novel higher-order cycloadditions with excellent periselectivity and enantiocontrol.[6] Cinchona alkaloids are privileged scaffolds in catalysis,[7] and their functional diversity and adjustability have paved the way for realizing the potential of such stereoselective higher-order cycloadditions.[8]

Hence, in 2017, the first organocatalytic enantioselective higher-order cycloadditions were developed, facilitated by cinchona alkaloid primary amine catalysts.[8a] It was demonstrated that cross- and linear-dienamine-activated 2-cycloalkenones react with tropone and various heptafulvenes to provide the corresponding [6+4], [4+2], or [8+2] cycloadducts (Scheme 1). In addition to the stereocontrol offered by the catalyst used (**1a**, **1b**), it was shown that the periselectivity could be tuned by varying the ring size of the cyclic enones and by changing the substitution pattern on the polyene. Complete periselectivity was achieved in most cases,

Received: October 20, 2020
Published: January 8, 2021

https://dx.doi.org/10.1021/jacs.0c10966

Scheme 1. Organocatalytic Dienamine Activation of Cycloalkenones and Selected Examples of Their Cycloadditions with Tropone and Heptafulvenes

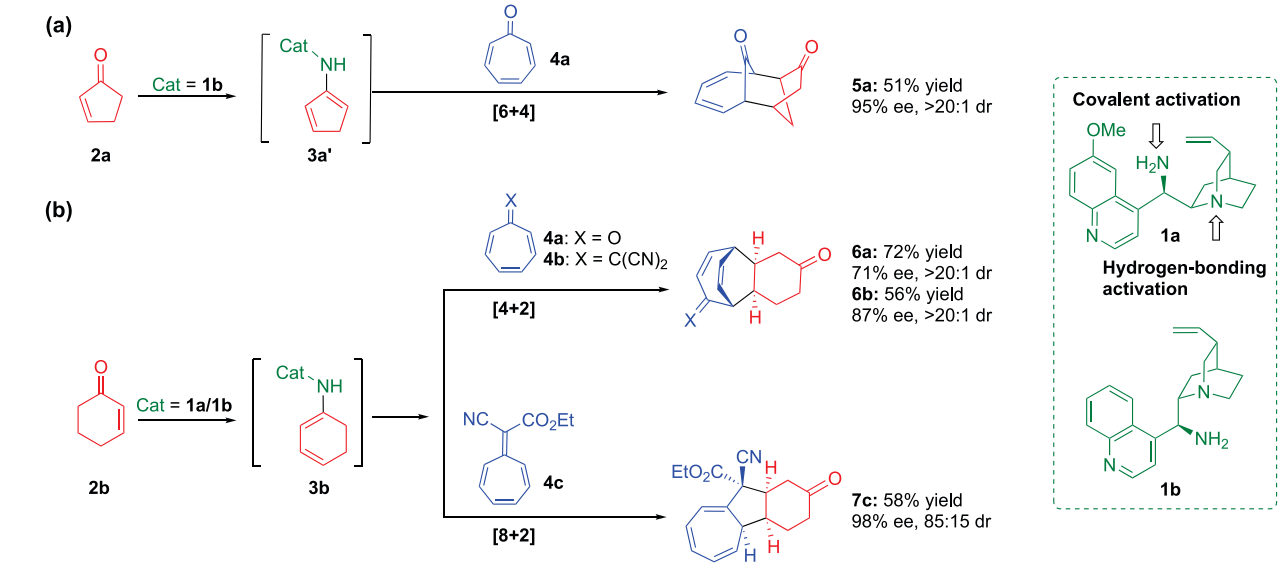

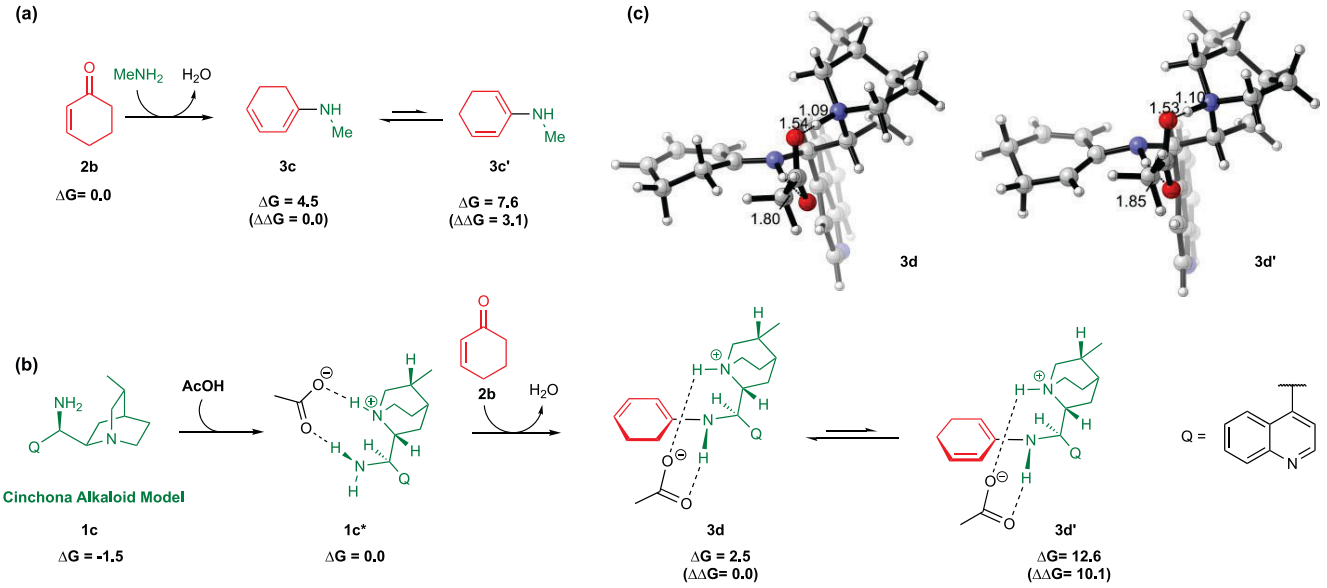

Figure 1. Relative stabilities of cross and linear dienamines with (a) *N*-methylamine and (b) cinchona alkaloid primary amine catalyst **1c**. (c) Optimized structures of **3d** and **3d′**. All energies are in kcal/mol, and distances are in Å.

and the cycloadducts were furnished with exceptional diastereo- and enantiocontrol.

Previously, we have carried out extensive computational and experimental investigations into the [6+4] cycloaddition between 2-cyclopentenone **2a** and tropone **4a** (Scheme 1a),[9] and we have now focused our attention toward explaining what governs the remarkable change in [8+2] vs [4+2] periselectivity observed in the reactions of 2-cyclohexenone **2b** with tropone and heptafulvenes.

The cinchona alkaloid primary-amine-catalyzed cycloadditions of 2-cyclohexenone with tropone or different heptafulvenes display fundamental differences in favored reaction paths, depending on the substituents present on the polyene reaction partner. Tropone **4a** and dicyano−heptafulvene **4b** both react with 2-cyclohexenone **2b**, catalyzed by **1a**, to produce exclusively the [4+2] cycloadducts **6a** and **6b**, in moderate to good yields, high diastereoselectivities, and good enantioselectivities (Scheme 1b, top). In contrast, applying the same reaction conditions to cyanoester-heptafulvene **4c** leads exclusively to the formation of the corresponding [8+2] cycloadduct **7c** in good yield and high stereoselectivity (Scheme 1b, bottom).

We describe new cooperative computational and experimental studies that elucidate the factors that determine chemo-, regio-, and stereoselectivity of these higher-order cycloadditions.

RESULTS AND DISCUSSION

To elucidate the observed changes in peri- and stereoselectivities, detailed mechanistic investigations of the possible [4+2] and [8+2] cycloadditions of tropone/heptafulvenes and linear dienamines **3c** and **3d** were performed with the range-separated density functional from the Head-Gordon group,

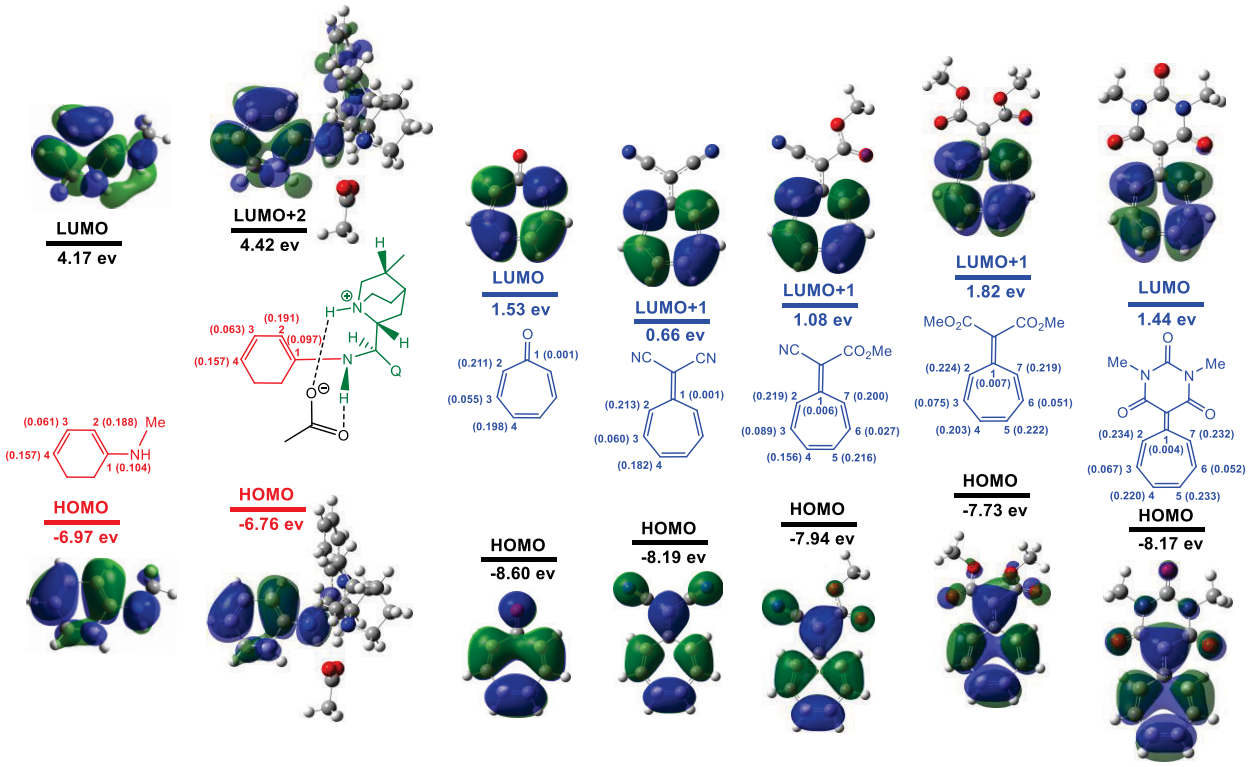

Figure 2. HF/6-31G(d) computation of the FMOs on DFT-optimized structures. Numbers in parentheses are sums of squares of the HOMO (linear dienamine) or LUMO coefficients at the corresponding carbon atoms.

ωB97X-D[10]/6-311++G(d,p),[11]SMD(toluene)[12]//ωB97X-D/6-31G(d),SMD(toluene), using Gaussian 09.[13] Detailed computational methods and results are given in the Supporting Information.

Formation of Cross and Linear Dienamines. Our mechanistic investigation was initiated by comparing the relative stabilities of the possible cross and linear dienamines that can result from the condensation of the cinchona alkaloid primary amine catalyst **1a** with 2-cyclohexenone **2b**. The catalyst **1a** was first simplified to *N*-methylamine (Figure 1a) to save the cost of calculation for the mechanistic study.[14] The formation of the corresponding linear dienamine **3c** is endergonic by 4.5 kcal/mol. The cross dienamine **3c′**, formed from **2b** and *N*-methylamine, is less stable than the linear dienamine by 3.1 kcal/mol. When the *N*-methylamine catalyst is replaced with a slightly truncated version (methyl replacing the vinyl) of the cinchona alkaloid primary amine catalyst under acidic conditions (acetic acid is important for obtaining results that are consistent with experiment,[8a] and the quinuclindinium−acetate ion pair is maintained in the calculations), this difference in stability becomes even more pronounced, with a preference of 10.1 kcal/mol for the linear dienamine intermediate **3d** over the cross dienamine **3d′** (Figure 1b). This result is consistent with empirical studies in which no [6+4] cycloaddition products arising from cross dienamine **3d′** (Figure 1c) and heptafulvenes were observed. Both the [8+2] and the [4+2] cycloadditions of 2-cyclohexenone **2b** with heptafulvenes catalyzed by **1c** thus proceed through the same linear dienamine intermediate **3d**.

Mechanistic Study. Next, the mechanisms of the [8+2] vs [4+2] cycloadditions of linear dienamine **3d** (Scheme S1 in Supporting Information) with tropone/heptafulvenes were investigated.

The computed frontier molecular orbitals (FMOs) of the nucleophilic dienamine and the relatively electrophilic heptafulvenes are displayed in Figure 2. The HOMO of the linear dienamine **3d** is strongly polarized toward C2 and C4. The HOMO coefficient is slightly larger at C2 than at C4; however, interaction of an electrophile at the C2 position suffers antibonding secondary interactions. Consequently, C4 of the diene becomes bonded to C2 of the heptafulvene, which has the largest LUMO/LUMO+1 coefficient.

[4+2] Cycloaddition of 2-Cyclohexenone and Tropone/Dicyano−heptafulvene. The free energy profiles of the [4+2] and [8+2] cycloadditions of 2-cyclohexenone **2b** with tropone **4a** and dicyanoheptafulvene **4b** are depicted in Figure 3a. The linear dienamine **3d** and tropone form a reactant complex **8a** with an increased free energy of 4.5 kcal/mol due to the unfavorable entropy of association. To maximize the overlap of the dienamine and tropone, no hydrogen bond is formed between the tropone oxygen and the protonated quinuclidine nitrogen of the catalyst. The first C−C bond formation, affording **9a**, proceeds through transition state (TS) **TSI_a** with a free energy of 26.2 kcal/mol. The bifunctional mode of **TSI_a**, with a hydrogen-bonding interaction between the tropone oxygen and the protonated quinuclidine, was also calculated and gave a 9.8 kcal/mol higher energy than the ion-pair mode (Figure S15). Different cycloadducts can form from intermediate **9a**. The [8+2] cycloadduct **10a**, produced via **TSII_a**, has the lowest energy barrier of 23.6 kcal/mol and thus forms readily. However, **10a** can revert to **9a** and then through **TSIII_a** form intermediate **11a**. This allows for equilibration to ultimately furnish the more stable [4+2] product **6a**, with a reverse barrier of 21.1 kcal/mol (**10a**→**TSIII_a**). The possibility of [6+4] cyclo-

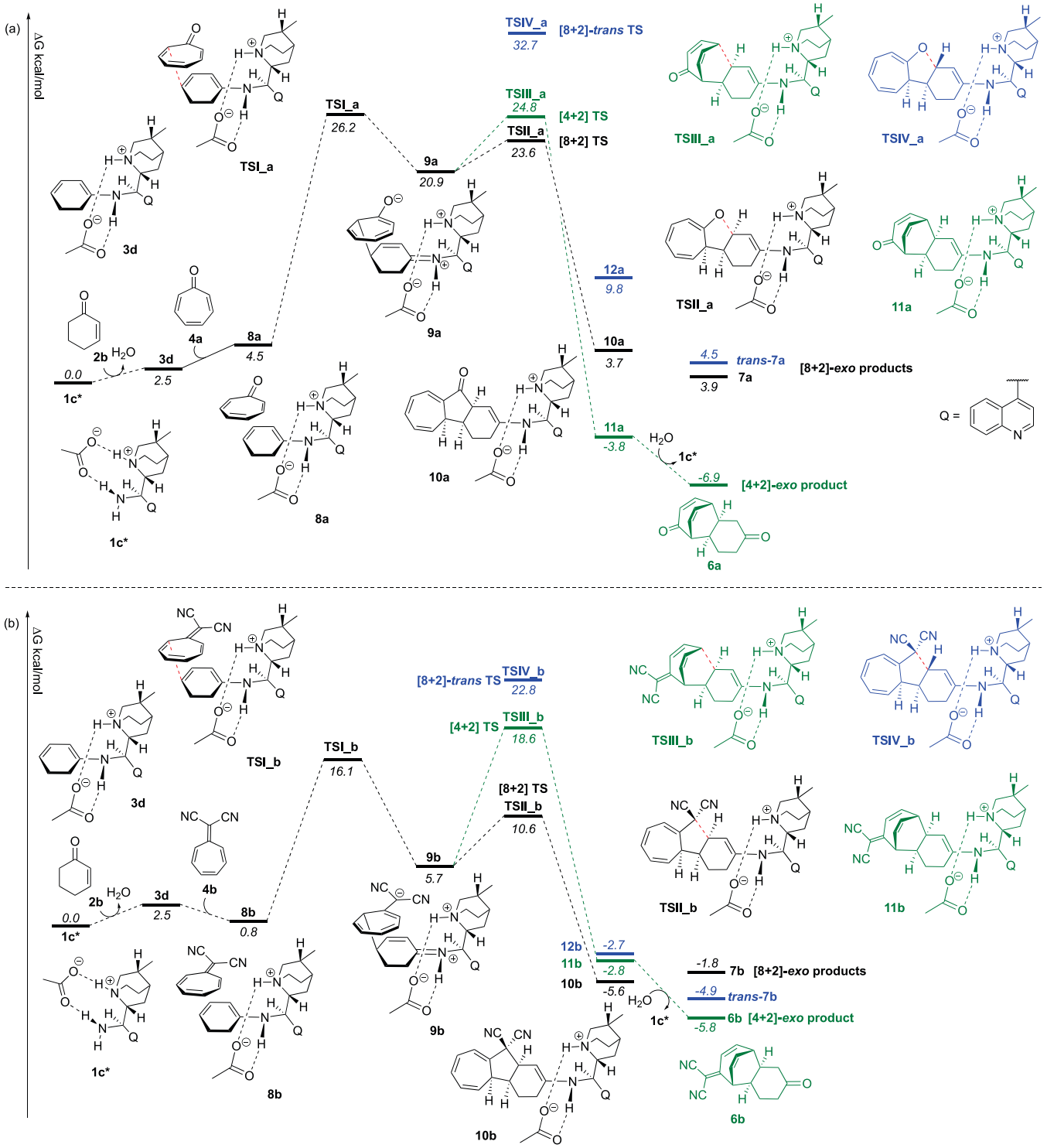

Figure 3. Free energy profiles of the [4+2] (green) and [8+2] (black and blue) cycloadditions of 2-cyclohexenone with (a) tropone **4a** and (b) dicyano−heptafulvene **4b**. All energies are in kcal/mol, with Grimme correction for entropy and Head-Gordon correction for enthalpy (frequency cutoff is 100.0 cm^{-1}).

adducts was also explored; however, the corresponding TSs were found to be significantly higher in energy.

The energy profile for the cycloaddition of 2-cyclohexenone **2b** and dicyano−heptafulvene **4b** (Figure 3b) is similar to that of tropone (Figure 3a). The linear dienamine **3d** and heptafulvene **4b** form reactant complex **8b**, with a free energy of 0.8 kcal/mol. The first C−C bond forms intermediate **9b** through **TSI_b**, with a free energy barrier of 16.1 kcal/mol. The bifunctional mode is 12.2 kcal/mol less stable than the ion-pair mode **TSI_b** (Figure S16). The lowest energy barrier for the ring closure of **TSII_b** leads to [8+2] cycloadduct **10b**. However, also in this case a relatively low reverse barrier of 24.2 kcal/mol (**10b**→**TSIII_b**) is found to ultimately obtain the more stable and experimentally observed [4+2] product.

Next, the stereodetermining formation of the first C−C bond was analyzed. The *N*-methylamine model, **model**-*exo*-

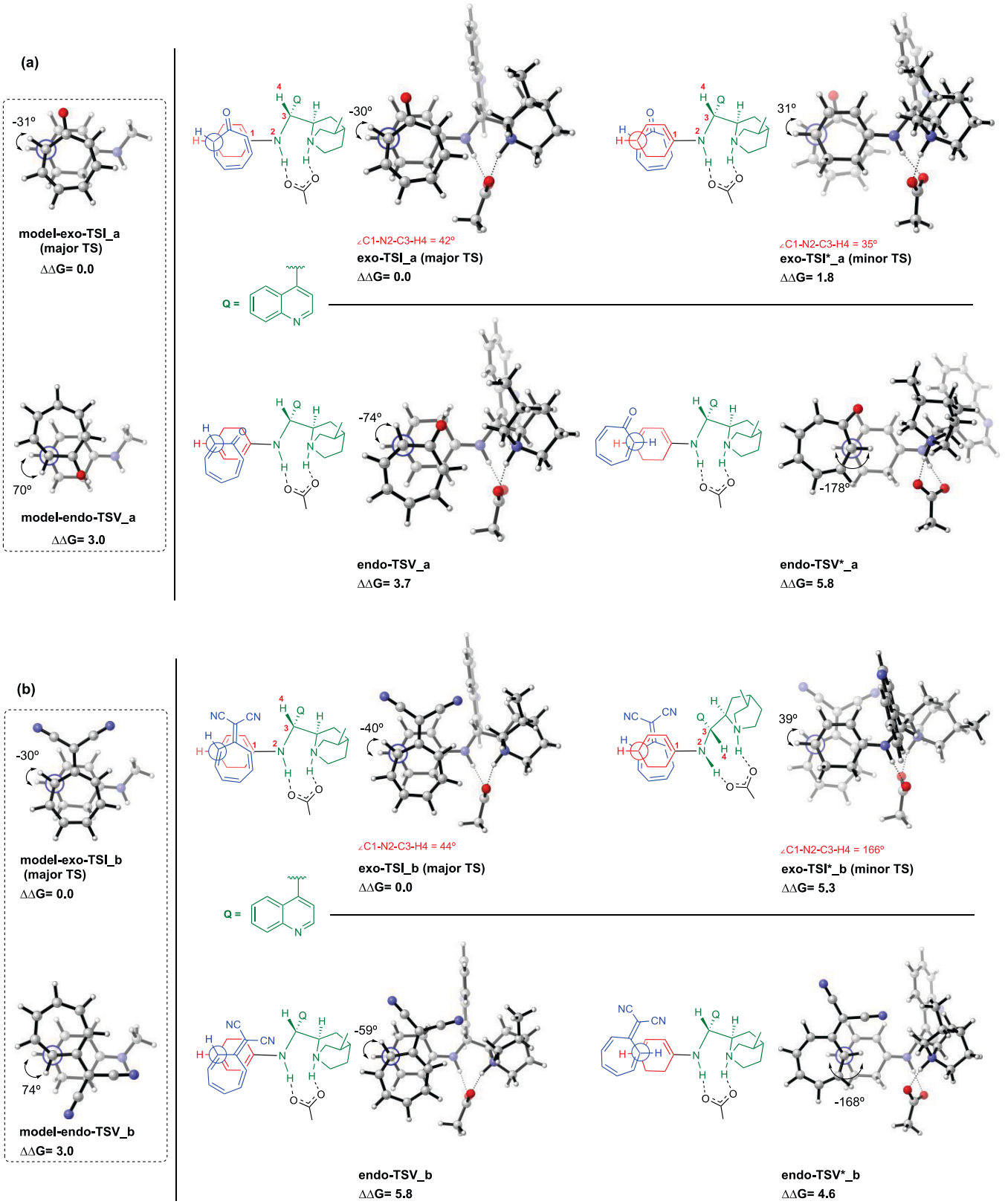

Figure 4. Diastereo- and enantiodetermining TS structures for (a) the [4+2] cycloaddition of 2-cyclohexanone and tropone and (b) the [4+2] cycloaddition of 2-cyclohexanone and dicyano−heptafulvene. All energies are in kcal/mol.

TSI_a, is calculated to be 3.0 kcal/mol more stable than **model**-*endo*-**TSV_a** due to ideal electrostatic and secondary orbital arrangement (Figure 4a, left). This energy difference becomes slightly larger in the presence of the cinchona alkaloid primary amine catalyst, for which the *exo*-**TSI_a** is favored by 3.7 kcal/mol (Figure 4a, middle). This is consistent with empirical data, since only the *exo*-[4+2] product is observed. Figure S5 displays a distortion/interaction analysis of TSI. The

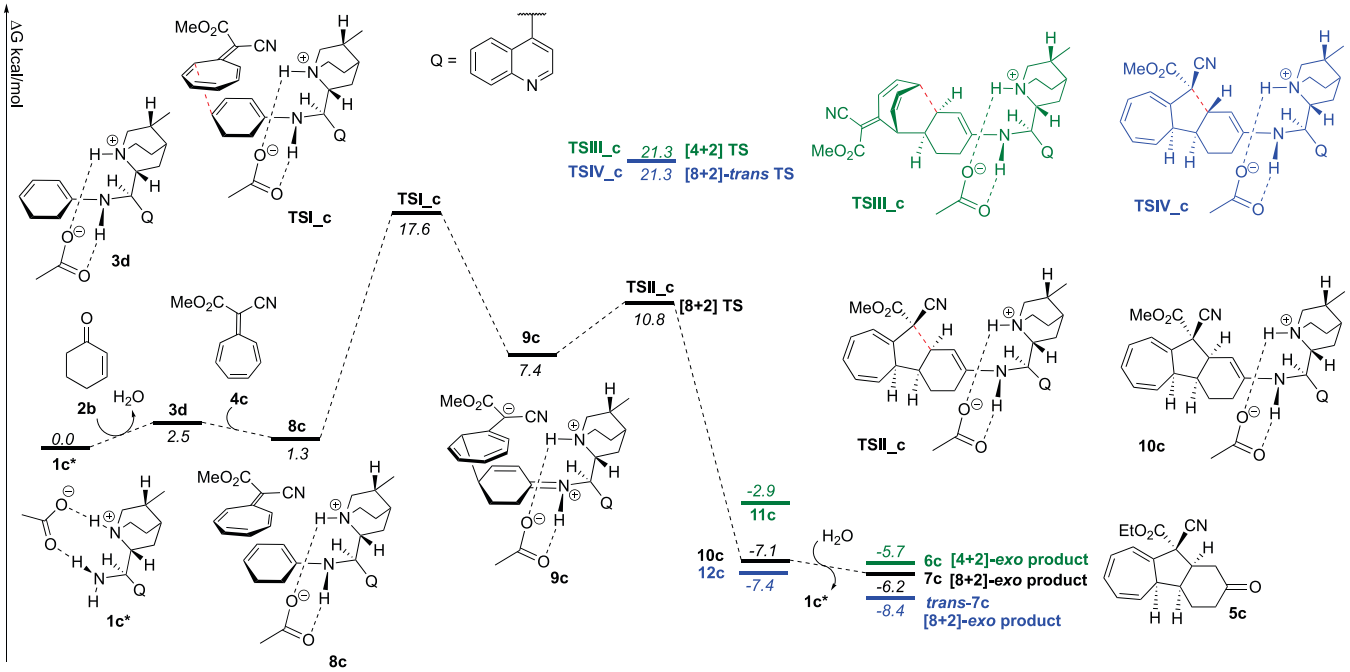

Figure 5. Free energy profiles of the [4+2] (green) and [8+2] (black and blue) cycloadditions of 2-cyclohexenone and cyanoester-heptafulvene **4c**. All energies are in kcal/mol and with Grimme correction for entropy and Head-Gordon correction for enthalpy (frequency cutoff is 100.0 cm^{-1}).

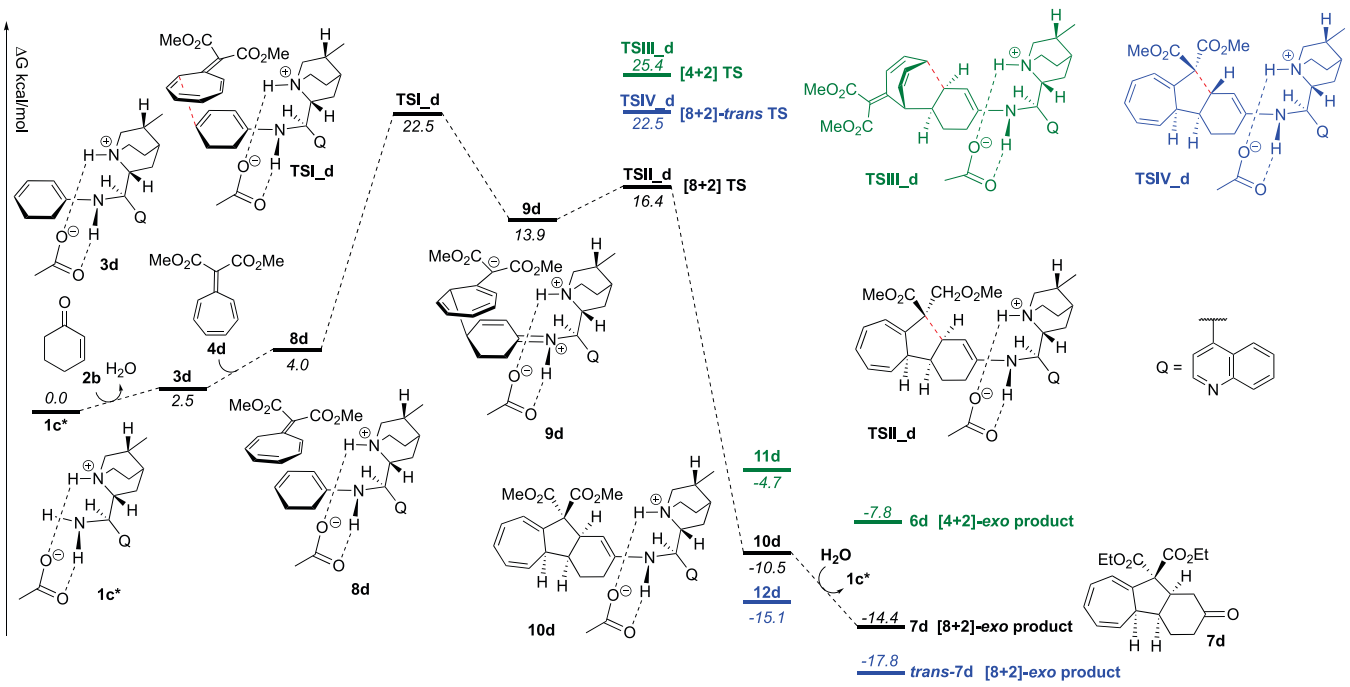

Figure 6. Free energy profiles of the [4+2] (green) and [8+2] (black and blue) cycloadditions of 2-cyclohexenone and diester-heptafulvene **4d**. All energies are in kcal/mol and with Grimme correction for entropy and Head-Gordon correction for enthalpy (frequency cutoff is 100.0 cm^{-1}).

enantioselectivity is determined by the steric interaction between tropone and the quinoline moiety of the catalyst. The TS with the two groups on opposite sides of the dienamine is favored by 1.8 kcal/mol and leads to the formation of the experimentally observed enantiomer of the product (Figure 4a, top right).

For heptafulvenes which possess larger groups on C8, the energy penalty of occupying the same side as the quinoline moiety leads to a conformational change in the catalyst, which results in an even larger energy difference of 5.3 kcal/mol between the two stereoisomeric transition states (Figure 4b, top, right). These calculations support the empirical observation that the [4+2] cycloadduct from dicyano-heptafulvene is furnished with higher enantioselectivity than that of tropone (71% ee vs 87% ee).

[8+2] Cycloaddition of 2-Cyclohexenone and Cyanoester-heptafulvene/Diester-heptafulvene. The free energy profiles of the [4+2] and [8+2] cycloadditions of 2-cyclohexenone **2b** with cyanoester-heptafulvene **4c** are depicted in Figure 5. Similar to the first two reactions, linear

dienamine **3d** and heptafulvene form reactant complex **8c**, with a free energy of 1.3 kcal/mol. Intermediate **9c** is then formed through **TSI_c**, with a free energy barrier of 17.6 kcal/mol. The [8+2] adduct **10c** again has the lowest barrier of formation through **TSII_c**, with a free energy of 10.8 kcal/mol. However, as opposed to the cycloadditions of tropone and dicyano−heptafulvene, the reverse reaction from **10c** is higher in energy, with a barrier of 28.4 kcal/mol (**10c**→ **TSIIIc**). Consequently, a kinetic control process governs the reaction, and only the initially formed [8+2] cycloadduct **7c** is obtained.

To further elucidate the effect of the heptafulvene substituents on the periselectivity, the free energy profiles of the [4+2] and [8+2] cycloadditions of 2-cyclohexenone **2b** and diester-heptafulvene **4d** were calculated (Figure 6). Dienamine **3d** and heptafulvene **4d** form a less stable reactant complex **8d**, with a free energy of 4 kcal/mol. The first C−C bond formation through **TSI_d** affords intermediate **9d**, with a free energy barrier of 22.5 kcal/mol. The [8+2] cycloadduct **10d** is then readily formed, through **TSII_d** with a free energy of 16.4 kcal/mol. As in the case for cyanoester-heptafulvene **4c**, the barriers from **10d** to **TSIII_d** and **TSIV_d** are too high (35.9 and 33.0 kcal/mol) for the reverse reaction to occur. Additionally, the [8+2] product is even the thermodynamically favored product compared to the [4+2] cycloadduct.

Despite previous efforts, the reaction of the diester-heptafulvene **4d** had not been observed experimentally. However, encouraged by the calculations predicting that diester-heptafulvene **4d** should follow a reaction path similar to that of cyanoester-heptafulvene **4c**, the reaction was revisited. Since the diester-heptafulvene **4d** was calculated to react significantly slower than the cyanoester-heptafulvene (22.5 kcal/mol vs 17.6 kcal/mol), a stoichiometric amount of cinchona alkaloid primary amine **1a** was employed. We were pleased to find that the [8+2] cycloadduct **7d** was obtained in 78% yield and 89% ee as a single diastereoisomer after a prolonged reaction time of 4 days (Scheme 2). However, we

Scheme 2. [8+2] Cycloaddition of 2-Cyclohexenone with Diester-heptafulvene 4d

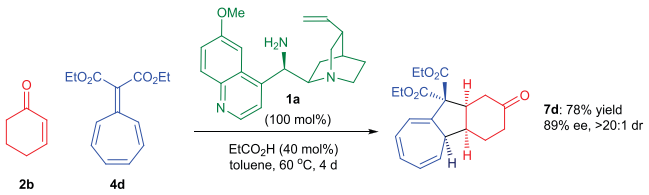

do note the disparities between the relatively low activation barrier of 22.5 kcal/mol and the rather harsh reaction conditions. Product formation is observed under catalytic conditions (20 mol% of **1a**), however, due to inherent instability of the [8+2] cycloadduct **7d**, the stochiometric amount of **1a** was required to obtain sufficient product for analytical purposes. Generally, the above experimental results are consistent with computational prediction. Product formation is also observed under catalytic conditions (20 mol% of **1a**); however, due to the inherent instability of the [8+2] cycloadduct **7d**, a stoichiometric amount of the catalyst was applied in order to obtain sufficient product for analytical purposes.

[8+2]-*trans* Cycloaddition of 2-Cyclohexenone and Barbiturate-heptafulvene/Thiobarbiturate-heptafulvene. This result prompted us to investigate not only diester-heptafulvene **4d** but also barbiturate- and thiobarbiturate-heptafulvenes **4e** and **4f** in their cycloadditions with 2-cyclohexenone **2b** catalyzed by cinchona alkaloid primary amine **1a**. The results of these reactions are shown in Scheme 3. The [8+2] cycloadduct **7e** from barbiturate-heptafulvene **4e**

Scheme 3. [8+2] Cycloadditions of Barbiturate- and Thiobarbiturate-heptafulvenes 4e and 4f with 2-Cyclohexenone 2b Catalyzed by Cinchona Alkaloid Primary Amine 1a

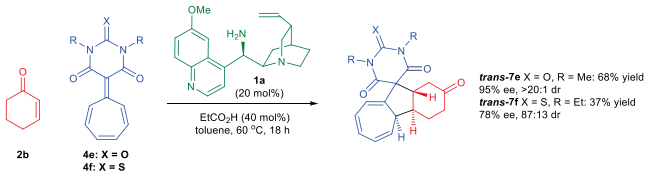

was obtained in 68% yield, >20:1 dr, and 95% ee, while the thio-derivative **4f** afforded the cycloadduct **7f** in lower yield and stereoselectivity but with perfect periselectivity.

Interestingly, single-crystal X-ray diffraction data obtained from cycloadduct *trans*-**7e** revealed that the major diastereoisomer of the product contains a *trans*-junction of the 5,6-fused bicycle. This contrasts with the *cis*-stereochemical relationship previously established for the major diastereoisomer of cyanoester cycloadduct **7c**.

Additional DFT calculations were performed to study the reason for the formation of the [8+2] cycloadducts with a *trans*-junction of the 5,6-fused bicycle. In the case of the barbiturate-heptafulvene **4e** (Figure 7), the free energy barrier of the first C−C bond formation is 16.2 kcal/mol through **TSI_e**. From intermediate **9e**, [8+2] cycloadduct **10e** can form readily with a free energy of 10.7 kcal/mol through **TSII_e**. However, reversal to intermediate **9e** will result in the formation of the experimentally observed, thermodynamically more stable diastereoisomer ***trans*-7e**, with both newly formed C−C bonds now in equatorial conformations on the cyclohexenone ring.

Diastereo- and enantiodetermining TS structures for the [8+2] cycloadditions of cyanoester, diester, and barbiturate-heptafulvenes with 2-cyclohexenone are depicted in Figures S2−S4. In all cases, the lowest energy TS leads to the experimentally observed product.

A complete mechanistic overview (Scheme S1) and CYLView graphics of all the transition states are summarized in the Supporting Information, and all corresponding relative free energies of the possible [4+2], [8+2], and [8+2]-*trans* products in the cycloadditions of 2-cyclohexenone with tropone and heptafulvenes are depicted in Figure S6. We summarize in Figure 8 the relative free energies and kinetic activation barriers for the reactions studied here.

CONCLUSION

The mechanisms and origins of chemo- and stereoselectivities of the organocatalytic [8+2] vs [4+2] cycloadditions between 2-cyclohexenone and tropone/heptafulvenes have been studied with DFT computations and experimental investigations. Two truncated versions of the catalyst, using a simple *N*-methylamine $MeNH_2$ and a simplified (Me for vinyl) cinchona alkaloid primary amine catalyst, have been investigated to probe the influence of substituents on the reaction. In all cases,

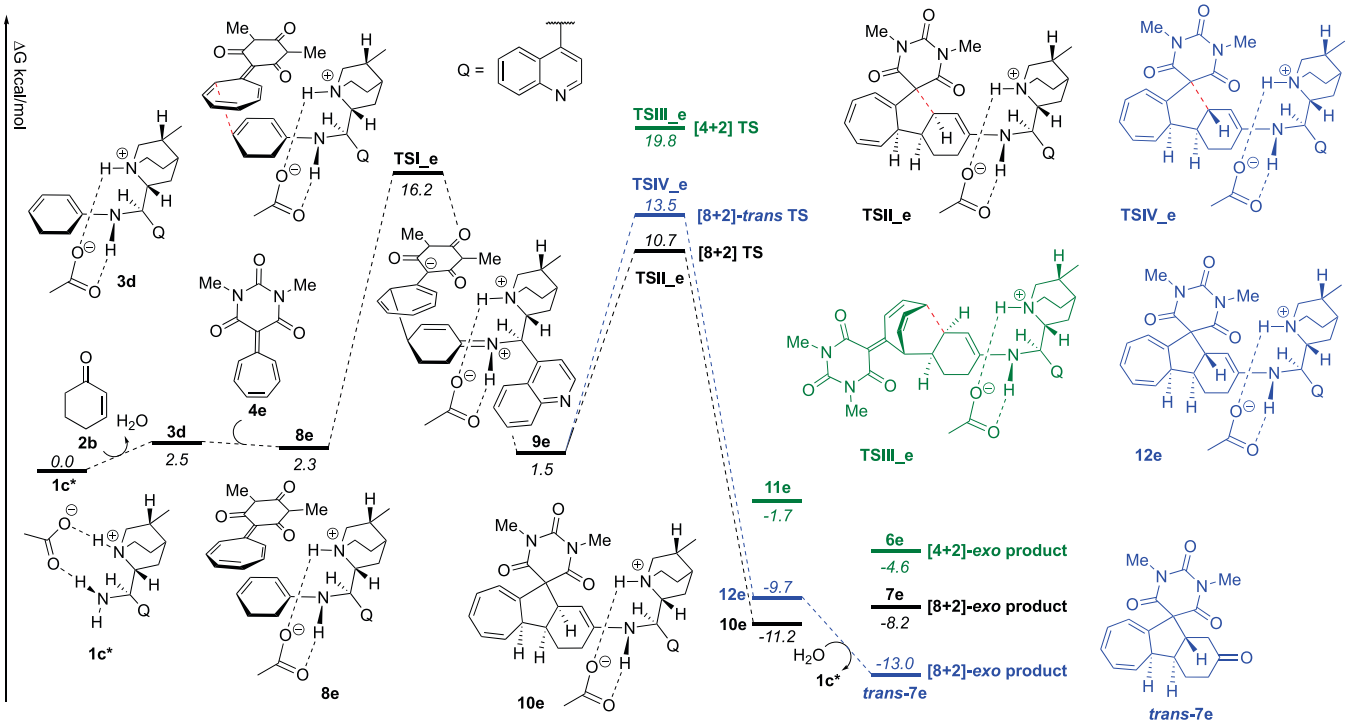

Figure 7. Free energy profiles of the [4+2] (green) and [8+2] (black and blue) cycloadditions of 2-cyclohexenone and barbiturate-heptafulvene **4e**. All energies are in kcal/mol and with Grimme correction for entropy and Head-Gordon correction for enthalpy (frequency cutoff is 100.0 cm^{-1}).

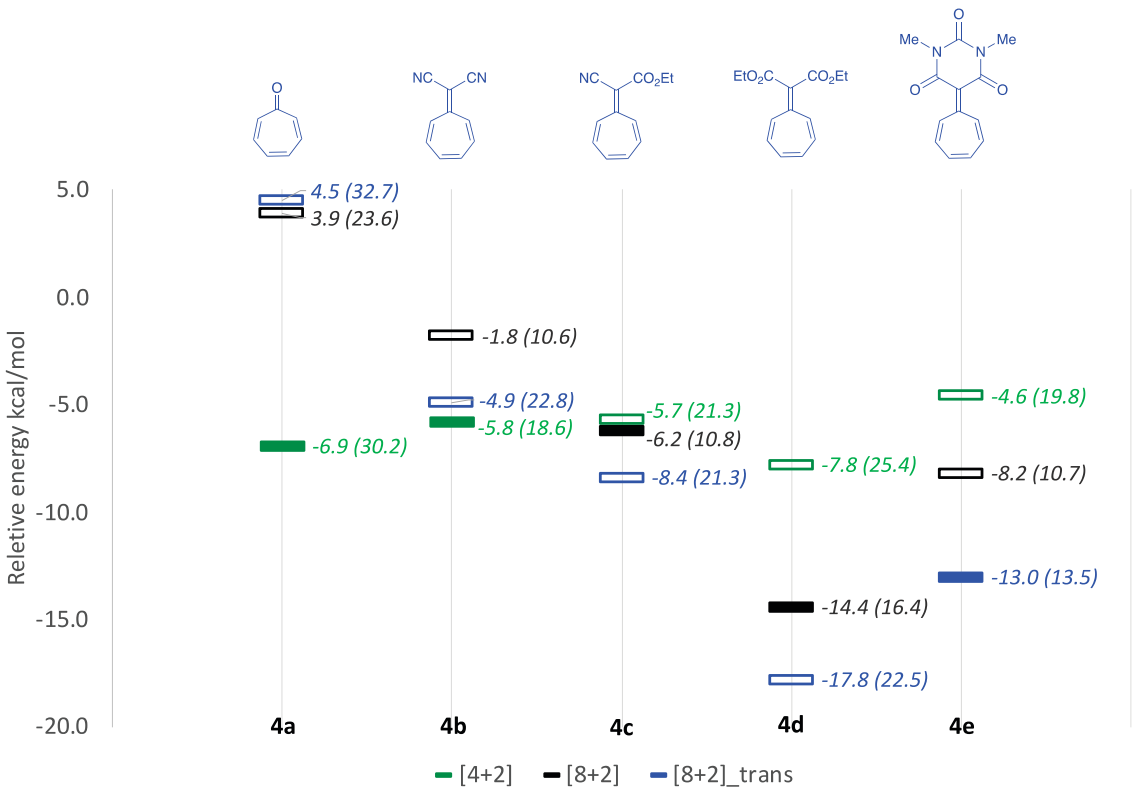

Figure 8. Gibbs free energies of [4+2] cycloadducts **6**, [8+2] cycloadducts **7**, and [8+2]-*trans* cycloadducts *trans*-**7** with respect to the respective starting materials (activation Gibbs free energies in parentheses). The experimentally observed products are marked as solid lines.

DFT calculations revealed that the cycloadditions proceed through stepwise mechanisms. The cinchona alkaloid primary amine catalyst generates an ion pair catalyst with the acid additive and leads to formation of the linear dienamine in preference to the cross dienamine intermediate. The [8+2] cycloaddition is much faster than the [4+2] cycloaddition due to the electron-rich tropone oxygen and heptafulvene C8 atoms with different substituents. The reversibility of the [8+2]

cycloadducts and the thermal stability of the [4+2] products determine the final periselectivity. For tropone and dicyanoheptafulvene, the most thermodynamically stable [4+2] products are observed due to a relatively favorable retro-cycloaddition barrier that allows for product equilibration. In contrast, the [8+2] cycloadducts from cyanoester-heptafulvene and diester-heptafulvene are formed under kinetic control due to a larger retro-cycloaddition barrier. In the cycloaddition of the barbiturate heptafulvene, the thermodynamically most stable *trans*-[8+2] cycloadduct is obtained as a result of a low retro-cycloaddition barrier and ultimately affords the product with a *trans*-5/6 fusion. Analysis of the stereoselectivity-determining first C−C bond formation revealed an energy preference for the *exo*-products over potential *endo*-products due to favorable electrostatic and secondary orbital arrangements. Additionally, a steric interaction between tropone/heptafulvenes and the quinoline of the catalyst was identified to be responsible for the discrimination of stereoisomeric transitions states leading to the experimentally observed major enantiomer of the corresponding products. These computational results are consistent with the excellent but variable selectivities observed experimentally with different heptafulvene derivatives.

■ ASSOCIATED CONTENT

Supporting Information

The Supporting Information is available free of charge at https://pubs.acs.org/doi/10.1021/jacs.0c10966.

Experimental procedures, X-ray crystallographic data, proposed mechanism, conformers of protonated cinchona alkaloid models, diastereo- and enantiodetermining TS structures, distortion/interaction analysis for the cycloaddition of 2-cyclohexanone and heptafulvenes, relative free energies of [4+2] cycloadducts **6**, [8+2] cycloadducts **7**, and [8+2]-*trans* cycloadducts *trans*-**7**, coordinates of all calculated structures, and product characterization data (PDF)

X-ray crystallographic data for *cis*-**13** (CIF)

■ AUTHOR INFORMATION

Corresponding Authors

Karl Anker Jørgensen − *Department of Chemistry, Aarhus University, DK-8000 Aarhus C, Denmark;* orcid.org/0000-0002-3482-6236; Email: kaj@chem.au.dk

K. N. Houk − *Department of Chemistry and Biochemistry, University of California, Los Angeles, California 90095, United States;* orcid.org/0000-0002-8387-5261; Email: houk@chem.ucla.edu

Authors

Xiangyang Chen − *Department of Chemistry and Biochemistry, University of California, Los Angeles, California 90095, United States;* orcid.org/0000-0002-6981-7022

Mathias Kirk Thøgersen − *Department of Chemistry, Aarhus University, DK-8000 Aarhus C, Denmark*

Limin Yang − *Department of Chemistry and Biochemistry, University of California, Los Angeles, California 90095, United States; College of Materials, Chemistry and Chemical Engineering, Hangzhou Normal University, Hangzhou 311121, China;* orcid.org/0000-0003-1021-3942

Rune F. Lauridsen − *Department of Chemistry, Aarhus University, DK-8000 Aarhus C, Denmark*

Xiao-Song Xue − *Department of Chemistry and Biochemistry, University of California, Los Angeles, California 90095, United States; State Key Laboratory of Elemento-Organic Chemistry, College of Chemistry, Nankai University, Tianjin 300071, China;* orcid.org/0000-0003-4541-8702

Complete contact information is available at: https://pubs.acs.org/10.1021/jacs.0c10966

Author Contributions

†X.C. and M.K.T. contributed equally to this work.

Notes

The authors declare no competing financial interest.

■ ACKNOWLEDGMENTS

K.A.J. thanks Villum Investigator Grant (no. 25867), the Carlsberg Foundation "Semper Ardens", and Aarhus University. Computations were performed on the Hoffman2 cluster at UCLA and the Extreme Science and Engineering Discovery Environment (XSEDE), which is supported by the National Science Foundation (OCI-1053575). We are grateful for financial support of the UCLA work from the National Science Foundation (CHE-1764328 to K.N.H.).

■ REFERENCES

(1) (a) Diels, O.; Alder, K. Synthesen in Der Hydroaromatischen Reihe. *Justus Liebigs Ann. Chem.* **1928**, *460*, 98−122. (b) Corey, E. J. Catalytic Enantioselective Diels−Alder Reactions: Methods, Mechanistic Fundamentals, Pathways, and Applications. *Angew. Chem., Int. Ed.* **2002**, *41*, 1650−1667. (c) Nicolaou, K. C.; Snyder, S. A.; Montagnon, T.; Vassilikogiannakis, G. The Diels−Alder Reaction in Total Synthesis. *Angew. Chem., Int. Ed.* **2002**, *41*, 1668−1698.

(2) (a) Hoffmann, R.; Woodward, R. B. Selection Rules for Concerted Cycloaddition Reactions. *J. Am. Chem. Soc.* **1965**, *87*, 2046−2048. (b) Woodward, R. B.; Hoffmann, R. Orbital Symmetries and endo/exo Relationships in Concerted Cycloadditions. *J. Am. Chem. Soc.* **1965**, *87*, 4388−4389. (c) Woodward, R. B.; Hoffmann, R. The Conservation of Orbital Symmetry. *Angew. Chem., Int. Ed. Engl.* **1969**, *8*, 781−932. (d) Woodward, R. B.; Hoffmann, R. *The Conservation of Orbital Symmetry*; Verlag Chemie GmbH, Academic Press, Inc.: Germany, 1970.

(3) (a) Woodward, R. B.; Katz, T. J. The Mechanism of the Diels-Alder Reaction. *Tetrahedron* **1959**, *5*, 70−89. (b) Dewar, M. J. S.; Olivella, S.; Stewart, J. J. P. Mechanism of the Diels-Alder Reaction: Reactions of Butadiene with Ethylene and Cyanoethylenes. *J. Am. Chem. Soc.* **1986**, *108*, 5771−5779. (c) Goldstein, E.; Beno, B.; Houk, K. N. Density Functional Theory Prediction of the Relative Energies and Isotope Effects for the Concerted and Stepwise Mechanisms of the Diels-Alder Reaction of Butadiene and Ethylene. *J. Am. Chem. Soc.* **1996**, *118*, 6036−6043.

(4) (a) Takeshita, H.; Wada, Y.; Mori, A.; Hatsui. The Cycloaddition Reaction of Isobenzofuran With Some Tropones. *Chem. Lett.* **1973**, *2*, 335−336. (b) Li, P.; Yamamoto, H. Formal Synthesis of Platencin. *Chem. Commun.* **2010**, *46*, 6294−6295. (c) Li, P.; Yamamoto, H. Lewis Acid Catalyzed Inverse-Electron-Demand Diels-Alder Reaction of Tropones. *J. Am. Chem. Soc.* **2009**, *131*, 16628−16629. (d) Houk, K. N.; Luskus, L. J.; Bhacca, N. S. The Novel Double [6+4] Cycloaddition of Tropone to Dimethylfulvene. *J. Am. Chem. Soc.* **1970**, *92*, 6392−6394. (e) Truce, W. E.; Lin, C.-I. M. Stereoselective Sulfene-Tropone Cycloadditions and Stereospecific Thermolysis of Resulting Adducts. *J. Am. Chem. Soc.* **1973**, *95*, 4426−4428. (f) Trost, B. M.; Seoane, P. R. [6+3] Cycloaddition to Nine-Membered Ring Carbocycles. *J. Am. Chem. Soc.* **1987**, *109*, 615−617. (g) Trost, B. M.; McDougall, P. J.; Hartmann, O.; Wathen, P. T. Asymmetric Synthesis of Bicyclo[4.3.1]decadienes and Bicyclo[3.3.2]-

decadienes via [6+3] Trimethylenemethane Cycloaddition with Tropones. *J. Am. Chem. Soc.* **2008**, *130*, 14960−14961. (h) Garst, M. E.; Roberts, V. A.; Houk, K. N.; Rondan, N. G. Even" Regioselectivity in [6+4] Cycloadditions of Unsymmetrical Tropones with Dienes. *J. Am. Chem. Soc.* **1984**, *106*, 3882−3884.

(5) (a) Rigby, J. H.; Fleming, M. Construction of the Ingenane Core Using an Fe(III) or Ti(IV)Lewis Acid-Catalyzed Intramolecular [6+4] Cycloaddition. *Tetrahedron Lett.* **2002**, *43*, 8643−8646. (b) Rigby, J. H.; Ateeq, H. S.; Charles, N. R.; Cuisiat, S. V.; Ferguson, M. D.; Henshilwood, J. A.; Krueger, A. C.; Ogbu, C. O.; Short, K. M.; Heeg, M. J. Metal-Promoted Higher-Order Cycloaddition Reactions. Stereochemical, Regiochemical, and Mechanistic Aspects of the [6π+4π] Reaction. *J. Am. Chem. Soc.* **1993**, *115*, 1382−1396. (c) Rigby, J. H.; Ateeq, H. S. Synthetic Studies on Transition-Metal-Mediated Higher Order Cycloaddition Reactions: Highly Stereoselective Construction of Substituted Bicyclo[4.4.1]undecane Systems. *J. Am. Chem. Soc.* **1990**, *112*, 6442−6443. (d) Rigby, J. H.; Henshilwood, J. A. Transition Metal Template Controlled Cycloaddition Reactions. An Efficient Chromium(0)-mediated [6π+2π] Cycloaddition. *J. Am. Chem. Soc.* **1991**, *113*, 5122−5123.

(6) (a) Kallweit, I.; Schneider, C. Brønsted Acid Catalyzed [6+2]-Cycloaddition of 2-Vinylindoles with in Situ Generated 2-Methide-2H-pyrroles: Direct, Catalytic, and Enantioselective Synthesis of 2,3-Dihydro-1H-pyrrolizines. *Org. Lett.* **2019**, *21*, 519−523. (b) Balanna, K.; Madica, K.; Mukherjee, S.; Ghosh, A.; Poisson, T.; Besset, T.; Jindal, G.; Biju, A. T. N-Heterocyclic Carbene Catalyzed Formal [6+2] Annulation Reaction via Cross-Conjugated Aza-Trienolate Intermediates. *Chem. - Eur. J.* **2020**, *26*, 818−822. (c) Bertuzzi, G.; Thøgersen, M. K.; Giardinetti, M.; Vidal-Albalat, A.; Simon, A.; Houk, K. N.; Jørgensen, K. A. Catalytic Enantioselective Hetero-[6+4] and -[6+2] Cycloadditions for the Construction of Condensed Polycyclic Pyrroles, Imidazoles, and Pyrazoles. *J. Am. Chem. Soc.* **2019**, *141*, 3288−3297. (d) McLeod, D.; Cherubini-Celli, A.; Sivasothirajah, N.; McCulley, C. H.; Christensen, M. L.; Jørgensen, K. A. Enantioselective 1,3-Dipolar [6+4] Cycloaddition of Pyrylium Ions and Fulvenes towards Cyclooctanoids. *Chem. - Eur. J.* **2020**, *26*, 11417−11422. (e) Donslund, B. S.; Monleón, A.; Palazzo, T. A.; Christensen, M. L.; Dahlgaard, A.; Erickson, J. D.; Jørgensen, K. A. Organocatalytic Enantioselective Higher-Order Cycloadditions of In Situ Generated Amino isobenzofulvenes. *Angew. Chem., Int. Ed.* **2018**, *57*, 1246−1250. (f) Gao, Z.; Wang, C.; Zhou, L.; Yuan, C.; Xiao, Y.; Guo, H. Phosphine-Catalyzed [8+2]-Annulation of Heptafulvenes with Allenoates and Its Asymmetric Variant: Construction of Bicyclo[5.3.0]decane Scaffold. *Org. Lett.* **2018**, *20*, 4302−4305. (g) Wang, S.; Rodriguez-Escrich, C.; Fianchini, M.; Maseras, F.; Pericas, M. A. Diastereodivergent Enantioselective [8+2] Annulation of Tropones and Enals Catalyzed by *N*-Heterocyclic Carbenes. *Org. Lett.* **2019**, *21*, 3187−3192. (h) He, C.; Li, Z.; Zhou, H.; Xu, J. Stereoselective [8+2] Cycloaddition Reaction of Azaheptafulvenes with α-Chloro Aldehydes via *N*-Heterocyclic Carbene Catalysis. *Org. Lett.* **2019**, *21*, 8022−8026. (i) Frankowski, S.; Skrzyńska, A.; Albrecht, L. Inverting the Reactivity of Troponoid Systems in Enantioselective Higher-order Cycloaddition. *Chem. Commun.* **2019**, *55*, 11675−11678. (j) Manzano, R.; Romaniega, A.; Prieto, L.; Díaz, E.; Reyes, E.; Uria, U.; Carrillo, U.; Vicario, J. L. γ-Substituted Allenic Amides in the Phosphine-Catalyzed Enantioselective Higher Order Cycloaddition with Azaheptafulvenes. *Org. Lett.* **2020**, *22*, 4721−4725. (k) Donslund, B. S.; Jessen, N. I.; Bertuzzi, G.; Giardinetti, M.; Palazzo, T. A.; Christensen, M. L.; Jørgensen, K. A. Catalytic Enantioselective [10+4] Cycloadditions. *Angew. Chem., Int. Ed.* **2018**, *57*, 13182−13186. (l) McLeod, D.; Thøgersen, M. K.; Jessen, N. I.; Jørgensen, K. A.; Jamieson, C. S.; Xue, X.-S.; Houk, K. N.; Liu, F.; Hoffmann, R. Expanding the Frontiers of Higher-Order Cycloadditions. *Acc. Chem. Res.* **2019**, *52*, 3488−3501. (m) Bertuzzi, G.; McLeod, D.; Mohr, L.-M.; Jørgensen, K. A. Organocatalytic Enantioselective 1,3-dipolar [6+4] Cycloadditions of Tropone. *Chem. - Eur. J.* **2020**, *26*, 15491. (n) Wang, S.; Rodríguez-Escrich, C.; Pericàs, M. A. Catalytic Asymmetric [8+2] Annulation Reactions Promoted by a Recyclable Immobilized Isothiourea. *Angew. Chem., Int. Ed.* **2017**, *56*, 15068−15072.

(7) (a) Marcelli, T.; Hiemstra, H. Cinchona Alkaloids in Asymmetric Organocatalysis. *Synthesis* **2010**, *8*, 1229−1279. (b) Yoon, T. P.; Jacobsen, E. N. Privileged Chiral Catalysts. *Science* **2003**, *299*, 1691−1693. (c) Melchiorre, P. Cinchona-based Primary Amine Catalysis in the Asymmetric Functionalization of Carbonyl Compounds. *Angew. Chem., Int. Ed.* **2012**, *51*, 9748−9770. (d) Tian, S.-K.; Chen, Y.; Hang, J.; Tang, L.; McDaid, P.; Deng, L. Asymmetric Organic Catalysis with Modified Cinchona Alkaloids. *Acc. Chem. Res.* **2004**, *37*, 621−631. (e) Jew, S.-S.; Park, H.-G. Cinchona-based Phase-transfer Catalysts for Asymmetric Synthesis. *Chem. Commun.* **2009**, *46*, 7090−7103. (f) Bergonzini, G.; Vera, S.; Melchiorre, P. Cooperative Organocatalysis for the Asymmetric γ-Alkylation of α-Branched Enals. *Angew. Chem., Int. Ed.* **2010**, *49*, 9685−9688. (g) Oliva, C. G.; Silva, A. M. S.; Resende, D. I. S. P.; Paz, F. A. A.; Cavaleiro, J. A. S. Highly Enantioselective 1,4-Michael Additions of Nucleophiles to Unsaturated Aryl Ketones with Organocatalysis by Bifunctional Cinchona Alkaloids. *Eur. J. Org. Chem.* **2010**, *2010*, 3449−3458. (h) Duan, J.; Li, P. Asymmetric Organocatalysis Mediated by Primary Amines Derived from Cinchona Alkaloids: Recent Advances. *Catal. Sci. Technol.* **2014**, *4*, 311−320.

(8) (a) Mose, R.; Preegel, G.; Larsen, J.; Jakobsen, S.; Iversen, E. H.; Jørgensen, K. A. Organocatalytic Stereoselective [8+2] and [6+4] Cycloadditions. *Nat. Chem.* **2017**, *9*, 487−492. (b) Zhou, Z.; Wang, Z.-X.; Zhou, Y.-C.; Xiao, W.; Ouyang, Q.; Du, W.; Chen, Y.-C. Switchable Regioselectivity in Amine-catalysed Asymmetric Cycloadditions. *Nat. Chem.* **2017**, *9*, 590−594. (c) Yang, Y.; Jiang, Y.; Du, W.; Chen, Y.-C. Asymmetric Cross [10+2] Cycloadditions of 2-Alkylidene-1-indanones and Activated Alkenes under Phase-Transfer Catalysis. *Chem. - Eur. J.* **2020**, *26*, 1754−1758.

(9) Yu, P.; He, C. Q.; Simon, A.; Li, W.; Mose, R.; Thøgersen, M. K.; Jørgensen, K. A.; Houk, K. N. Organocatalytic [6+4] Cycloadditions via Zwitterionic Intermediates: Chemo-, Regio-, and Stereoselectivities. *J. Am. Chem. Soc.* **2018**, *140*, 13726−13735.

(10) Chai, J. D.; Head-Gordon, M. Long-range Corrected Hybrid Density Functionals with Damped Atom-atom Dispersion Corrections. *Phys. Chem. Chem. Phys.* **2008**, *10*, 6615−6620.

(11) (a) Krishnan, R.; Binkley, J. S.; Seeger, R.; Pople, J. A. Self-consistent Molecular Orbital Methods. XX. A Basis set for Correlated Wave Functions. *J. Chem. Phys.* **1980**, *72*, 650−654. (b) Ditchfield, R.; Hehre, W. J.; Pople, J. A. Self-Consistent Molecular-Orbital Methods. IX. An Extended Gaussian-Type Basis for Molecular-Orbital Studies of Organic Molecules. *J. Chem. Phys.* **1971**, *54*, 724−728. (c) Hehre, W. J.; Ditchfield, R.; Pople, J. A. Self-Consistent Molecular Orbital Methods. XII. Further Extensions of Gaussian—Type Basis Sets for Use in Molecular Orbital Studies of Organic Molecules. *J. Chem. Phys.* **1972**, *56*, 2257−2261. (d) Hariharan, P. C.; Pople, J. A. The Influence of Polarization Functions on Molecular Orbital Hydrogenation Energies. *Theor. Chim. Acta* **1973**, *28*, 213−222.

(12) (a) Tomasi, J.; Mennucci, B.; Cammi, R. Quantum Mechanical Continuum Solvation Models. *Chem. Rev.* **2005**, *105*, 2999−3094. (b) Marenich, A. V.; Cramer, C. J.; Truhlar, D. G. Universal Solvation Model Based on Solute Electron Density and on a Continuum Model of the Solvent Defined by the Bulk Dielectric Constant and Atomic Surface Tensions. *J. Phys. Chem. B* **2009**, *113*, 6378−6396.

(13) Frisch, M. J.; Trucks, G. W.; Schlegel, H. B.; Scuseria, G. E.; Robb, M. A.; Cheeseman, J. R.; Scalmani, G.; Barone, V.; Mennucci, B.; Petersson, G. A.; Nakatsuji, H.; Caricato, M.; Li, X.; Hratchian, H. P.; Izmaylov, A. F.; Bloino, J.; Zheng, G.; Sonnenberg, J. L.; Hada, M.; Ehara, M.; Toyota, K.; Fukuda, R.; Hasegawa, J.; Ishida, M.; Nakajima, T.; Honda, Y.; Kitao, O.; Nakai, H.; Vreven, T.; Montgomery, J. A., Jr.; Peralta, J. E.; Ogliaro, F.; Bearpark, M. J.; Heyd, J.; Brothers, E. N.; Kudin, K. N.; Staroverov, V. N.; Kobayashi, R.; Normand, J.; Raghavachari, K.; Rendell, A. P.; Burant, J. C.; Iyengar, S. S.; Tomasi, J.; Cossi, M.; Rega, N.; Millam, N. J.; Klene, M.; Knox, J. E.; Cross, J. B.; Bakken, V.; Adamo, C.; Jaramillo, J.; Gomperts, R.; Stratmann, R. E.; Yazyev, O.; Austin, A. J.; Cammi, R.; Pomelli, C.; Ochterski, J. W.; Martin, R. L.; Morokuma, K.;

Zakrzewski, V. G.; Voth, G. A.; Salvador, P.; Dannenberg, J. J.; Dapprich, S.; Daniels, A. D.; Farkas, Ö.; Foresman, J. B.; Ortiz, J. V.; Cioslowski, J.; Fox, D. J. *Gaussian 09*, revision C.01; Gaussian, Inc.: Wallingford, CT, USA, 2009.

(14) Lifchits, O.; Mahlau, M.; Reisinger, C. M.; Lee, A.; Fares, C.; Polyak, I.; Gopakumar, G.; Thiel, W.; List, B. The Cinchona Primary Amine-catalyzed Asymmetric Epoxidation and Hydroperoxidation of α,β-Unsaturated Carbonyl Compounds with Hydrogen Peroxide. *J. Am. Chem. Soc.* **2013**, *135*, 6677−6693.